Numerical Analysis of the Dynamics of Single and Double Spring-Pendulum Systems

Aaron Lewin and Paula Chen

Math 53 - Fall 2015

---

1 Introduction

The classic elastic pendulum is a mechanical system consisting of a mass hanging from a spring (**Figure 1a**). This single spring-pendulum system has been well-studied previously, and current literature shows that chaotic motion is possible given certain initial conditions, even without damping and when restricted to two dimensions ([2], [3], [4], [5], [6]).

In our investigation, we used Hamiltonian dynamics to model two different spring-pendulum systems in MATLAB. First, we confirmed that chaotic motion is possible in the classic single spring-pendulum system in two dimensions and without damping. Next, we modified the system by attaching the mass to two springs (**Figure 1b**) and tested to see how the dynamics change with the addition of this second spring to the system.

Some of the characteristics of chaotic motion include an unbounded, aperiodic orbit, sensitive dependence, and positive Lyapunov exponent ([1]). Therefore, in order to determine whether chaotic motion is possible in each our spring-pendulum systems, we tested for sensitive dependence via a log separation plot, calculated the Lyapunov exponents for various initial conditions, and created potential energy contour maps in order to better visualize the stability of various trajectories.

2 System Design

The single spring-pendulum system consists of a fixed mass hanging from a spring pendulum (**Figure 1a**). The double spring-pendulum system consists of a fixed mass hanging from two springs of equivalent natural lengths and with equivalent spring constants (**Figure 1b**). For simplicity, we assume that, in both systems, the springs can stretch but cannot bend and are

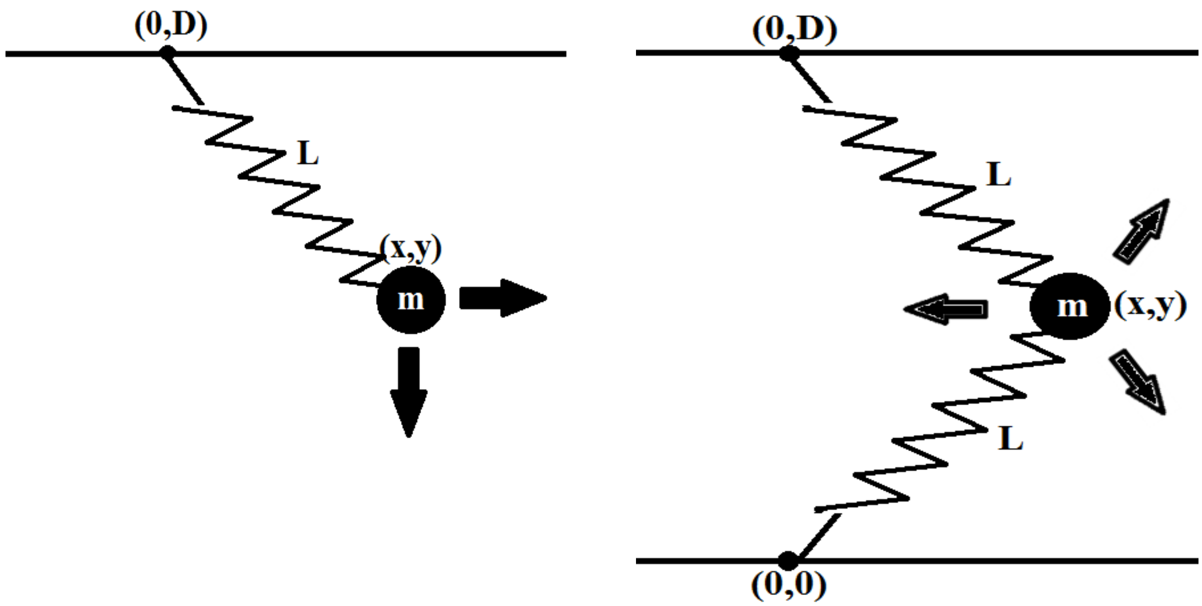

(a) Single Spring-Pendulum System

(b) Double Spring-Pendulum System

Figure 1: **Schematic diagram of the two spring-pendulum systems.**

of negligible mass and that the mass is free to move in two dimensions, i.e. has two degrees of freedom. We also assume that there are no damping forces acting on either system. Our system parameters were chosen semi-randomly based on convenience. Finally, in the double spring-pendulum system, we set $D < 2L$ in order to ensure that the the equilibrium point on the y-axis is unstable (i.e. the springs always buckle).

3 Derivation of the Hamiltonian Equations of Motion

Note that since we worked in Cartesian coordinates, the equations for the momenta and velocities could have been derived without the use of the Hamiltonian and instead simply with force equations, alone.

3.1 Single Spring-Pendulum System

Let the mass m have position (x, y) (where x, y are functions of time) and be hanging from a rigid, massless, undamped spring of natural length L and with spring constant k. Assume the spring is attached to the point $(0, D)$ above the ground. Let the acceleration due to gravity be g. (See **Figure 1a**.)

The kinetic energy (T) of the system is then given by:

$$T = \frac{m}{2} \cdot (velocity)^2 = \frac{m}{2}(\dot{x}^2 + \dot{y}^2)$$

And the potential energy (V) of the system is given by:

$$V = V_{spring} + V_{gravity} = \frac{k}{2}(\sqrt{x^2 + (y-D)^2} - L)^2 + mgy$$

From this, we have that the Lagrangian L is given by:

$$L = T - V = \frac{m}{2}(\dot{x}^2 + \dot{y}^2) - \frac{k}{2}(\sqrt{x^2 + (y-D)^2} - L)^2 - mgy$$

The generalized momenta p_i are then calculated to be:

$$p_x = \frac{\partial L}{\partial \dot{x}} = m\dot{x}$$
$$p_y = \frac{\partial L}{\partial \dot{y}} = m\dot{y}$$

Solving for $\dot{x}$ and $\dot{y}$ gives us:

$$\dot{x} = \frac{p_x}{m}$$
$$\dot{y} = \frac{p_y}{m}$$

Substituting in for $\dot{x}$ and $\dot{y}$ gives us that the Hamiltonian H is:

$$H = \frac{p_x^2}{m} + \frac{p_y^2}{m} - \frac{m}{2}((\frac{p_x}{m})^2 + (\frac{p_y}{m})^2) + \frac{k}{2}(\sqrt{x^2 + (y-D)^2} - L)^2 + mgy$$

Therefore, the Hamiltonian equations of motion for the single spring-pendulum system are:

$$\dot{x} = \frac{\partial H}{\partial p_x} = \frac{p_x}{m}$$
$$\dot{y} = \frac{\partial H}{\partial p_y} = \frac{p_y}{m}$$
$$\dot{p}_x = -\frac{\partial H}{\partial x} = -kx + kLx(x^2 + (y-D)^2)^{-1/2}$$
$$\dot{p}_y = -\frac{\partial H}{\partial y} = -k(y-D) + kL(y-D)(x^2 + (y-D)^2)^{-1/2} - mg$$

The Jacobean J for the single spring-pendulum system is then determined to be:

$$J = \begin{pmatrix} 0 & 0 & \frac{1}{m} & 0 \\ 0 & 0 & 0 & \frac{1}{m} \\ j_1 & j_2 & 0 & 0 \\ j_3 & j_4 & 0 & 0 \end{pmatrix}$$

where

$$j_1 = -k + kL(x^2 + (y-D)^2)^{-1/2} - kLx^2(x^2 + (y-D)^2)^{-3/2}$$
$$j_2 = -kLx(y-D)(x^2 + (y-D)^2)^{-3/2}$$
$$j_3 = -kLx(y-D)(x^2 + (y-D)^2)^{-3/2}$$
$$j_4 = -k + kL(x^2 + (y-D)^2)^{-1/2} - kL(y-D)^2(x^2 + (y-D)^2)^{-3/2}$$

3.2 Double Spring-Pendulum System

Let the mass m have position (x, y) (where x, y are functions of time) and be hanging from two rigid, massless, undamped springs, both of natural length L and with spring constant k. Assume one spring is attached to the point $(0, D)$ and the other spring is attached to the point $(0, 0)$, where $D < 2L$. Let the acceleration due to gravity be g. (See **Figure 1b**.)

The kinetic energy (T) of the system is then given by:

$$T = \tfrac{m}{2}(\dot{x}^2 + \dot{y}^2)$$

And the potential energy (V) of the system is given by:

$$V = \tfrac{k}{2}(\sqrt{x^2 + y^2} - L)^2 + \tfrac{k}{2}(\sqrt{x^2 + (y - D)^2} - L)^2 + mgy$$

From this, we have that the Lagrangian L is given by:

$$L = T - V = \tfrac{m}{2}(\dot{x}^2 + \dot{y}^2) - \tfrac{k}{2}(\sqrt{x^2 + y^2} - L)^2 - \tfrac{k}{2}(\sqrt{x^2 + (y - D)^2} - L)^2 - mgy$$

The generalized momenta p_i are then calculated to be:

$$p_x = \tfrac{\partial L}{\partial \dot{x}} = m\dot{x}$$
$$p_y = \tfrac{\partial L}{\partial \dot{y}} = m\dot{y}$$

Solving for $\dot{x}$ and $\dot{y}$ gives us:

$$\dot{x} = \tfrac{p_x}{m}$$
$$\dot{y} = \tfrac{p_y}{m}$$

Substituting in for $\dot{x}$ and $\dot{y}$ gives us that the Hamiltonian H is:

$$H = \tfrac{p_x^2}{m} + \tfrac{p_y^2}{m} - \tfrac{m}{2}((\tfrac{p_x}{m})^2 + (\tfrac{p_y}{m})^2) + \tfrac{k}{2}(\sqrt{x^2 + y^2} - L)^2 + \tfrac{k}{2}(\sqrt{x^2 + (y - D)^2} - L)^2 + mgy$$

Therefore, the Hamiltonian equations of motion for the double spring-pendulum system are:

$$\dot{x} = \tfrac{\partial H}{\partial p_x} = \tfrac{p_x}{m}$$
$$\dot{y} = \tfrac{\partial H}{\partial p_y} = \tfrac{p_y}{m}$$
$$\dot{p}_x = -\tfrac{\partial H}{\partial x} = -2kx + +kLx(x^2 + y^2)^{-1/2} + kLx(x^2 + (y - D)^2)^{-1/2}$$
$$\dot{p}_y = -\tfrac{\partial H}{\partial y} = -2ky + Dk + kLy(x^2 + y^2)^{-1/2} + +kL(y - D)(x^2 + (y - D)^2)^{-1/2} - mg$$

The Jacobean J for the double spring-pendulum system is then determined to be:

$$J = \begin{pmatrix} 0 & 0 & \frac{1}{m} & 0 \\ 0 & 0 & 0 & \frac{1}{m} \\ j_1 & j_2 & 0 & 0 \\ j_3 & j_4 & 0 & 0 \end{pmatrix}$$

where

$$j_1 = -2k + kL(x^2+y^2)^{-1/2} - kx^2L(x^2+y^2)^{-3/2} + kL(x^2+(y-D)^2)^{-1/2} - kx^2L(x^2+(y-D)^2)^{-3/2}$$

$$j_2 = -kLxy(x^2+y^2)^{-3/2} - kLx(y-D)(x^2+(y-D)^2)^{-3/2}$$

$$j_3 = -kLxy(x^2+y^2)^{-3/2} - kLx(y-D)(x^2+(y-D)^2)^{-3/2}$$

$$j_4 = kL[-\tfrac{2}{L} + (x^2+y^2)^{-1/2} - y^2(x^2+y^2)^{-3/2} + (x^2+(y-D)^2)^{-1/2} - (y-D)^2(x^2+(y-D)^2)^{-3/2}]$$

4 Numerical Experiments

We used MATLAB's ODE45 function to numerically solve the set of ODEs given by the Hamiltonian equations of motion. In order to perform numerical analysis of our two spring-pendulum systems, we have created three code files: LyapFind.m, Elastic_Pend_time1map.m, and Double_Spring_time1map.m.

Elastic_Pend_time1map.m and Double_Spring_time1map.m are function files that are called in LyapFind.m to calculate Lyapunov exponents using the Jacobean derivatives for the single and double spring-pendulum systems, respectively. Our code file LyapFind.m performs the following tasks for both the single spring and double spring systems:

- Performs a sensitive dependence test by creating a log plot of the separation of two paths that begin a small distance ϵ apart in each Cartesian coordinate; measuring the slope of the growth phase of these plots would result in a crude estimation of the Lyapunov exponent at the given initial condition
- Determines Lyapunov exponents more accurately by the re-orthogonalizing and repeated averaging method using Jacobean derivatives; the tested initial conditions and corresponding Lyapunov exponents are then written to a text file
- Creates an animation that plots the flow for a given set of initial conditions (plotted in white) and for a point starting a small distance ϵ away in each Cartesian coordinate (plotted in green) from these given initial conditions on a potential energy contour map
- Creates a Lyapunov exponent color plot that displays the Lyapunov exponents corresponding to each initial condition in an array of initial conditions tested

The program that we have created is highly interactive and allows the user to determine which functions they want to use by simply changing flag values and initial conditions. The flags determine which spring system to analyze as well as which operations (as described above) to run. Our program also simultaneously parses through several different initial conditions, which the user can specify prior to running the code.

Because of Liouville's Theorem, which states that Hamiltonian flows in $\mathbb{R}^{2n}$ are volume-preserving (i.e. the sum of all of the Lyapunov exponents is 0) ([1]), we expect the four

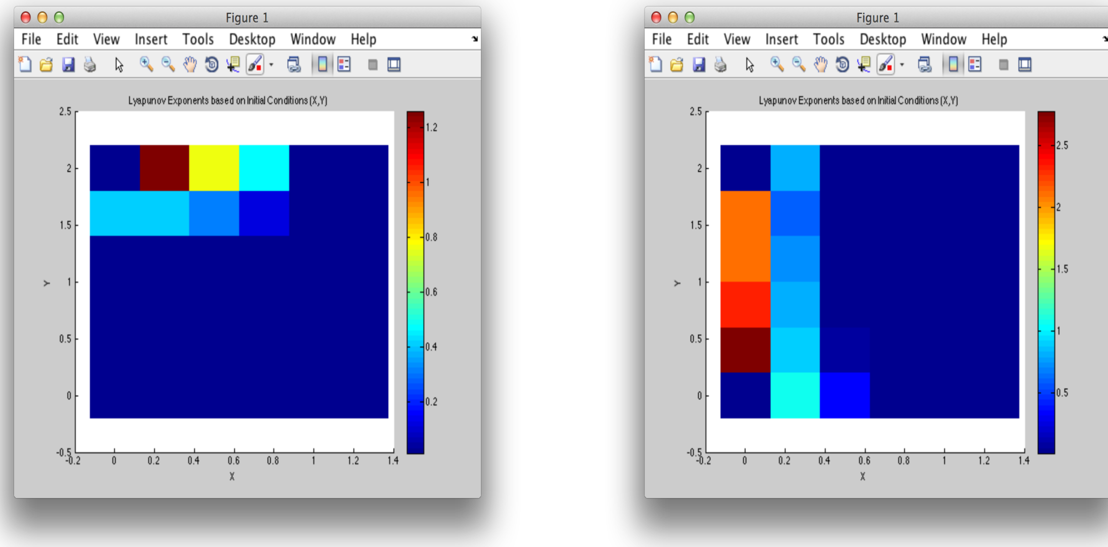

(a) Single Spring-Pendulum System

(b) Double Spring-Pendulum System

Figure 2: **Lyapunov Exponent Color Plots.** These color plots were generated from a set of 36 initial conditions.

Lyapunov exponents for each initial condition to sum to 0, where one Lyapunov exponent is positive, one is negative, and the remaining two are 0. Thus, we use the two Lyapunov exponents closest to 0 as a measure of error and report the maximum Lyapunov exponent as $h1\pm$(the absolute value of the larger of the two Lyapunov exponents closest to 0).

Also, note that for our sensitive dependence tests, we set $\epsilon = 1e - 8$.

4.1 Single Spring-Pendulum System

We tested 36 different initial positions ranging from $(0, 0)$ to $(1.25, 2)$. Out of these 36, we found that initial position $(0.1, 2)$ had the largest maximum Lyapunov exponent, which, using the Jacobean determinant method, was calculated to be 1.260641 ± 0.022734. **Figure 2a** shows that out of the 36 initial conditions tested, only a small portion of initial positions had strongly positive Lyapunov exponents (the positions at which the spring was stretched a large amount in the y-direction but only somewhat stretched in the x-direction). In general, we found that the less the spring was stretched in the y-direction, the less positive the maximum Lyapunov exponent was.

Figure 3 shows the potential energy contour map and log separation plot for the non-chaotic orbit starting at initial position $(1, 0)$. Using the Jacobean determinant method, the maximum Lyapunov exponent was calculated to be 0.018695 ± 0.015789 (approximately

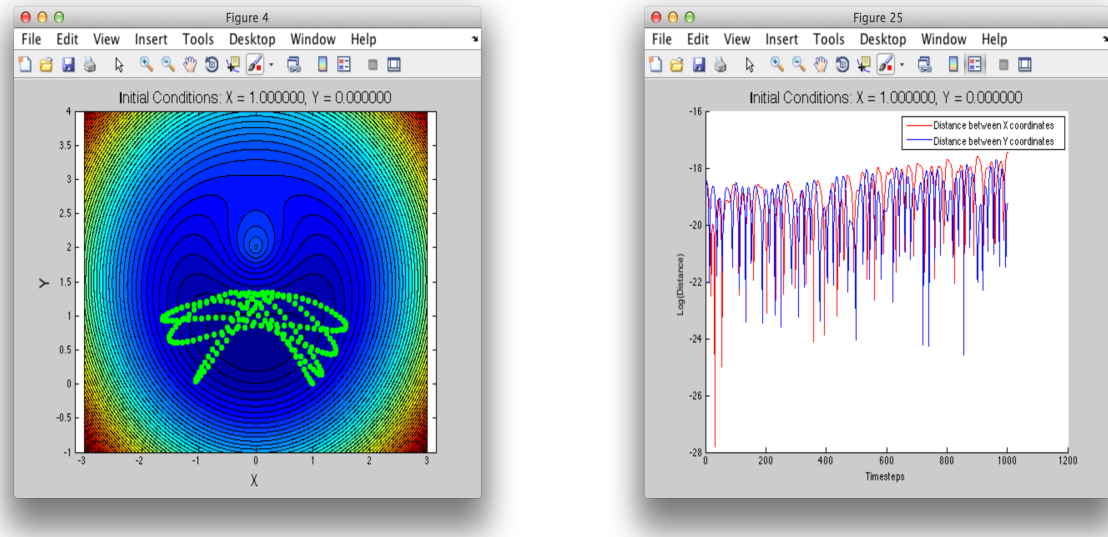

(a) Potential Energy Contour Map for $(1, 0)$ (b) Log Separation Plot for $(1, 0)$

Figure 3: **Plots for a Non-Chaotic Orbit in the Single Spring-Pendulum System.** The initial position for this orbit was $(1, 0)$. Using the Jacobean determinant method, the maximum Lyapunov exponent was calculated to be 0.018695 ± 0.015789 (approximately zero).

zero). The log separation plot (**Figure 3b**) shows essentially no growth phase, while the potential energy contour map (**Figure 3a**) shows no separation of the orbits beginning at initial positions $(1, 0)$ and $(1 + \epsilon, 0 + \epsilon)$. This orbit appears periodic, as we expect, and stays within one potential energy contour (i.e. the orbit can never have more potential energy than we give it initially). Therefore, since the Lyapunov exponent is approximately 0, there is no growth phase in the log separation plot (i.e. no sensitive dependence), and the orbit appears periodic, we conclude that the initial position $(1, 0)$ has a regular, non-chaotic orbit. Other orbits that had the same characteristics were also determined to be non-chaotic.

Figure 4 shows the potential energy contour map and log separation plot for the chaotic orbit starting at initial position $(0.3, 2)$. Using the Jacobean determinant method, the maximum Lyapunov exponent was calculated to be 0.755571 ± 0.030399 (> 0). The log separation plot (**Figure 4b**) shows a significant growth phase. However, the potential energy contour map (**Figure 4a**) shows no separation of the orbits beginning at initial positions $(0.3, 2)$ and $(0.3 + \epsilon, 2 + \epsilon)$, which is an unexpected result. In fact, none of the potential energy contour map animations for the orbits that we determined to be chaotic showed separation of the two orbits starting ϵ apart. It is possible that if we ran the animation for a longer period of time that we would eventually see the two orbits separate. It may also be that because we are limited by the numerical accuracy of of MATLAB that we do not see the separation that

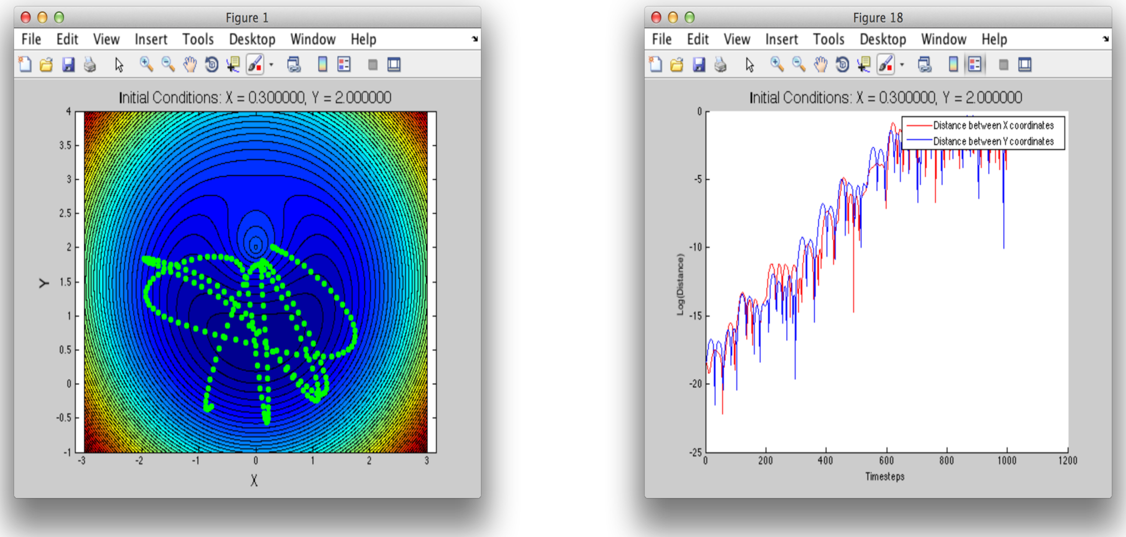

(a) Potential Energy Contour Map for $(0.3, 2)$ (b) Log Separation Plot for $(0.3, 2)$

Figure 4: **Plots for a Chaotic Orbit in the Single Spring-Pendulum System.** The initial position for this orbit was $(0.3, 2)$. Using the Jacobean determinant method, the maximum Lyapunov exponent was calculated to be 0.755571 ± 0.030399. (a) The potential energy contour map animation does not show separation of the two orbits starting ϵ apart.

we expect. Regardless, our animations do clearly demonstrate that these orbits with positive maximum Lyapunov exponents are not periodic. The orbit does however stay within one potential energy contour, which is consistent with the fact that the orbit can never exceed the amount of potential energy that we originally put into it (conservation of energy). Thus, we determined that orbits with positive Lyapunov exponents, significant growth phases in their log separation plots (i.e. sensitive dependence), and aperiodic orbits (e.g. that of the initial position $(0.3, 2)$) are chaotic.

4.2 Double Spring-Pendulum System

We tested 36 different initial positions ranging from $(0, 0)$ to $(1.25, 2)$. Out of these 36, we found that initial position $(0, 0.3)$ had the largest maximum Lyapunov exponent, which, using the Jacobean determinant method, was calculated to be 2.774417 ± 0.022406. **Figure 2b** shows that out of the 36 initial conditions tested, only a small portion of initial positions had strongly positive Lyapunov exponents (the positions at which the spring was stretched a large amount in the y-direction but has little to no stretching in the x-direction). In general, we found that the less stretched the spring was in the y-direction and the more stretched the spring was in the x-direction, the less positive the maximum Lyapunov exponent was.

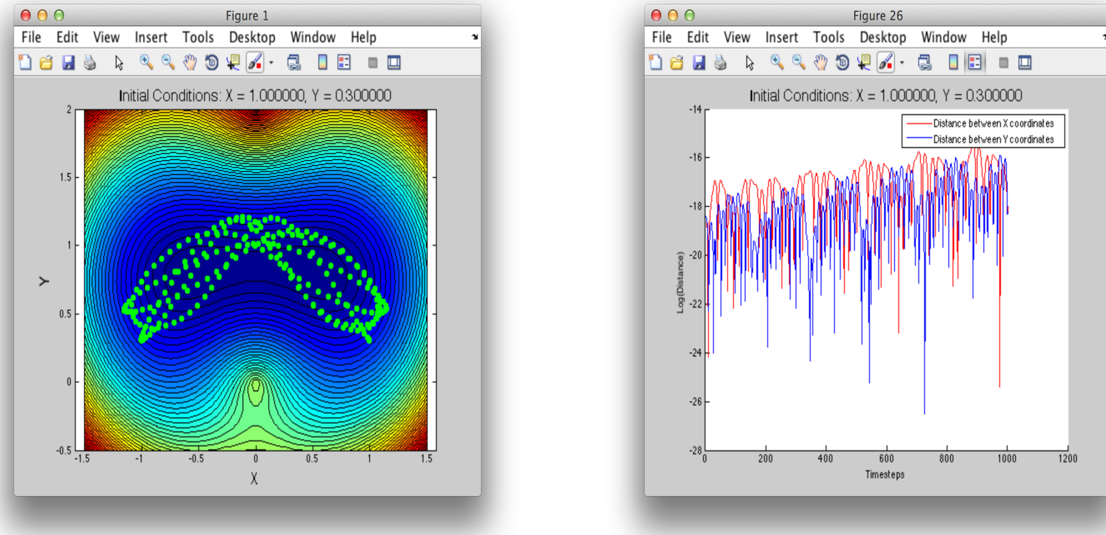

(a) Potential Energy Contour Map for $(1, 0.3)$ (b) Log Separation Plot for $(1, 0.3)$

Figure 5: **Plots for a Non-Chaotic Orbit in the Double Spring-Pendulum System.** The initial position for this orbit was $(1, 0.3)$. Using the Jacobean determinant method, the maximum Lyapunov exponent was calculated to be 0.027172 ± 0.021341 (approximately zero).

Figure 5 shows the potential energy contour map and log separation plot for the non-chaotic orbit starting at initial position $(1, 0.3)$. Using the Jacobean determinant method, the maximum Lyapunov exponent was calculated to be 0.027172 ± 0.021341 (approximately zero). The log separation plot (**Figure 5b**) shows essentially no growth phase, while the potential energy contour map (**Figure 5a**) shows no separation of the orbits beginning at initial positions $(1, 0.3)$ and $(1 + \epsilon, 0.3 + \epsilon)$. This orbit appears periodic, as we expect, and stays within one potential energy contour (i.e. the orbit can never have more potential energy than we give it initially). Therefore, since the Lyapunov exponent is approximately 0, there is no growth phase in the log separation plot (i.e. no sensitive dependence), and the orbit appears periodic, we conclude that the initial position $(1, 0.3)$ has a regular, non-chaotic orbit. Other orbits that had the same characteristics were also determined to be non-chaotic.

Figure 6 shows the potential energy contour map and log separation plot for the chaotic orbits starting at initial position $(0.1, 0.3)$ and $(0, 0.3)$. Using the Jacobean determinant method, the maximum Lyapunov exponent for the orbit of $(0.1, 0.3)$ was calculated to be 0.880759 ± 0.024596 (> 0) and the maximum Lyapunov exponent for the orbit of $(0, 0.3)$ was calculated to be 2.774417 ± 0.022406 (> 0). The log separation plots for both initial positions (**Figure 6b,d**) show a significant growth phase. However, the potential energy contour map

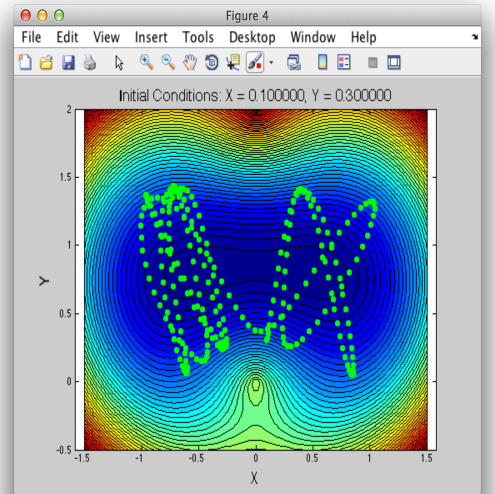

(a) Potential Energy Contour Map for $(0.1, 0.3)$

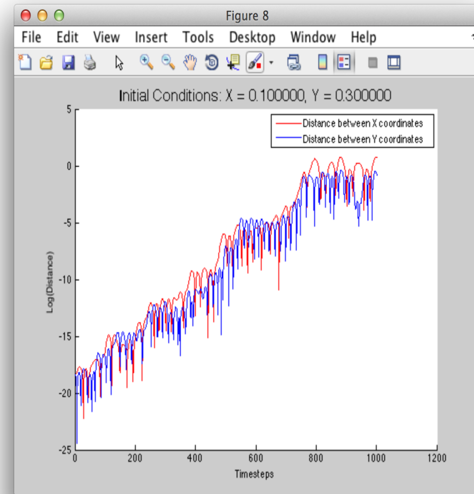

(b) Log Separation Plot for $(0.1, 0.3)$

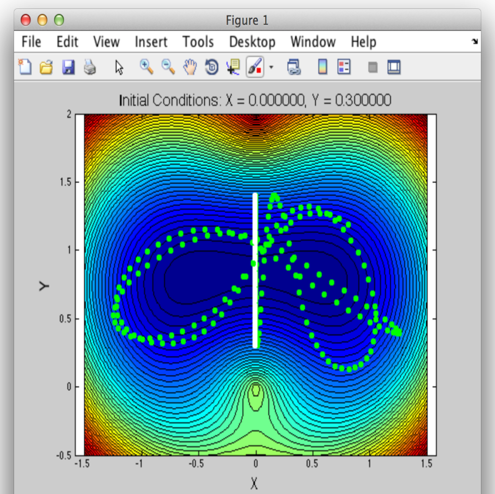

(c) Potential Energy Contour Map for $(0, 0.3)$

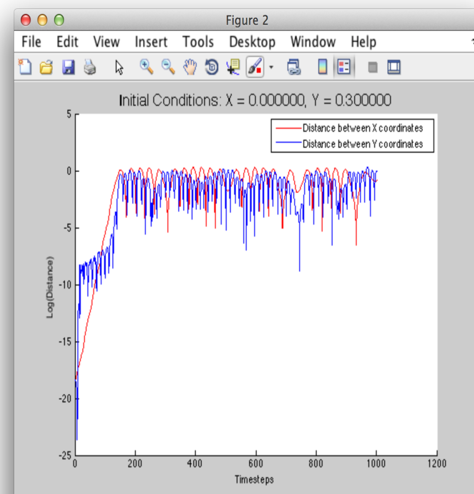

(d) Log Separation Plot for $(0, 0.3)$

Figure 6: **Plots for Chaotic Orbits in the Double Spring-Pendulum System.** (a, b) The initial position for this orbit was $(0.1, 0.3)$. Using the Jacobean determinant method, the maximum Lyapunov exponent was calculated to be 0.880759 ± 0.024596. (a) The potential energy contour map animation does not show separation of the two orbits starting ϵ apart. (c, d) The initial position for this orbit was $(0, 0.3)$. Using the Jacobean determinant method, the maximum Lyapunov exponent was calculated to be 2.774417 ± 0.022406. (c) The potential energy contour map animation clearly shows sensitive dependence.

(**Figure 6a**) for the orbit of $(0.1, 0.3)$ shows an aperiodic orbit with no sensitive dependence, similarly to the results we have seen in the single spring case. The potential energy contour map (**Figure 6c**) for the orbit of $(0, 0.3)$ shows an aperiodic orbit with sensitive dependence. Here, it may be important to note that $(0, 0.3)$ was the initial position with the largest maximum Lyapunov exponent out of the 36 initial positions we tested. This supports our idea that some of the chaotic orbits may not appear to show sensitive dependence on the potential energy contour map due to issues with numerical accuracy or the length of time for which we plotted the orbit; it may simply be that the orbit for $(0, 0.3)$ separated quickly enough for the separation to be visible on the potential energy contour map and that other chaotic orbits do not separate fast enough to be visible. Again, we did see that the orbits stayed within one potential energy contour, which is consistent with the fact that the orbit can have more potential energy than the amount that we originally put into it (conservation of energy). In general, all orbits with positive Lyapunov exponents, significant growth phases in their log separation plots (i.e. sensitive dependence), and aperiodic orbits were determined to be chaotic.

5 Conclusions

In both spring-pendulum systems, we found both regular and chaotic orbits, which is consistent with current literature on single spring-pendulum systems ([2],[4],[6]). We observed that, in either system, giving the mass a lot of potential energy, i.e. stretching the spring a lot, resulted in non-chaotic orbits. In general, the initial positions with chaotic orbits (i.e. strongly positive Lyapunov exponents) were nearby the equilibrium position of the spring, where the length of the spring was close to the natural length.

The main issue that we ran into in our experiments was that most of the orbits that we determined were chaotic based on their log separation plots and maximum Lyapunov exponents did not show sensitive dependence when their orbits were plotted on the potential energy contour maps. However, we strongly suspect that this discrepancy could be resolved by either running the plots of the orbits for a larger number of iterations or increasing the numerical accuracy of MATLAB's ODE45 solver, of which we have adjusted the tolerance to 1e-10 to accommodate our ϵ value of 1e-8 (the default tolerance level of the ODE45 function is 1e-6).

6 Future Directions

Based on our results, the logical next step would be to address the lack of observable sensitive dependence of chaotic orbits when plotted on the potential energy contour maps. In order to resolve this issue, we would need to increase the numerical accuracy of the ODE45 solver.

Another next step would be to improve the resolution of our Lyapunov exponent color plot by calculating the Lyapunov exponents for more initial conditions and over a larger range of initial positions. In order to accomplish this, we would also need to improve the efficiency of the part of our code that uses the Jacobean determinant method to find Lyapunov exponents. Currently, just running this part of the code for 36 initial conditions takes over an hour; therefore, making a higher resolution color plot would require a much smaller run time. Having a higher resolution Lyapunov exponent color plot may also help reveal if there exists some more concrete relationship between initial position, potential energy, and Lyapunov exponent value.

Some other interesting modifications to our system would be to see how damping changes the dynamics or to change our parameter values to either match real-life data or those used in current literature. With respect to the latter modification, it would be helpful to see if we could use our program to match the Lyapunov values reported in current literature. For example, Gonzalez, et al, reported that after non-dimensionalizing the parameters with the relation $c = 1 - \frac{mg}{kl}$, the trajectory with total energy 0.04875 had a maximum Lyapunov exponent converging to 0.037, and that this value was a sufficient indicator of chaos ([2]). Matching these values would help show that our calculated Lyapunov exponents are indeed reliable.

We could also try looking at Poincare sections as the majority of the other sources use this method to determine chaotic trajectories ([2], [3], [5], [6]). Finally, we could explore the dynamics of our two spring-pendulum systems in three dimensions to see what other behavior is possible.

7 References

[1] Kathleen T. Alligood, Tim D. Sauer, and James A. Yorke. *CHAOS: An Introduction to Dynamical Systems*. Textbooks in Mathematical Sciences. Springer, 1996. ISBN: 0387946772.

[2] R. Carretero-González, H. N. Nuñez-Yépez, and A. L. Salas-Brito. “Regular and chaotic behaviour in an extensible pendulum”. In: *Eur. J. Phys.* 15 (1994), pp. 139–148.

[3] R. Cuerno, A. F. Rañada, and J. J. Ruiz-Lorenzo. “Deterministic chaos in the elastic pendulum: A simple laboratory for nonlinear dynamics”. In: *American Journal of Physics* 60.1 (1992), pp. 73–79.

[4] Leah Ganis. *The Swinging Spring: Regular and Chaotic Motion*. 2013. URL: `http://math.arizona.edu/~gabitov/teaching/141/math_485/Midterm_Presentations/Elastic_Pedulum.pdf`.

[5] Peter Lynch. “The Swinging Spring: A Simple Model of Atmospheric Balance”. In: (2002).

[6] H. N. Nuñez-Yépez, A. L. Salas-Brito, and L. Vicente. “Onset of Chaos in an Extensible Pendulum”. In: *Physics Letters A* 145.2,3 (1990), pp. 101–105.